Advantages of multi-color fluorescent proteins for whole-body and *in vivo* cellular imaging

Robert M. Hoffman
AntiCancer, Inc.
7917 Ostrow Street
San Diego, California 92111
E-mail: all@anticancer.com

Abstract. The revolution of *in vivo* cancer biology enabled by fluorescent proteins is described. The high extinction coefficients, quantum yields, and unique spectral properties of fluorescent proteins have been taken advantage of in order to visualize, in real time, the important aspects of cancer in living animals, including tumor cell trafficking, invasion, metastasis, and angiogenesis. Fluorescent proteins enable whole-body imaging of tumors on internal organs. These multicolored proteins have allowed the color-coding of cancer cells growing *in vivo* with distinction of different cell types, including host from tumor, with single-cell resolution. © *2005 Society of Photo-Optical Instrumentation Engineers.* [DOI: 10.1117/1.1992485]

Keywords: imaging; fluorescence; image acquistion; image recording.

1 Introduction

1.1 GFP and Other Fluorescent Proteins as Imaging Agents

Green fluorescent protein (GFP) and related fluorescent proteins are a homologous family, having emission spectra from 442–645 nm.[1] This family of proteins range in size from 25–30 kDa and form internal chromophores that do not require cofactors or substrates in order to fluoresce. These fluorescent proteins have very high extinction coefficients ranging up to approximately $\acute{\varepsilon}=95,000$. In addition, they have very high quantum yields ranging up to 0.8.[2] These properties make fluorescent proteins exceedingly bright. GFP's large 2-photon absorption is important for *in vivo* applications.[2] Another important feature is the spectral distinction of many members of the family of fluorescent proteins. Therefore, a set of multi-color fluorescent proteins can be utilized simultaneously for multifunctional *in vivo* imaging. These properties make fluorescent proteins optimal for cellular imaging *in vivo*.

1.2 In Vivo Imaging with Fluorescent Proteins

The first use of fluorescent proteins in animals was to visualize cancer cells in fresh tissue.[3] Fluorescent proteins can be used to image essentially any type of cancer process including primary tumor growth, tumor cell motility, tumor cell invasion, intravasation, extravasation, metastatic seeding, metastatic colonization, angiogenesis, cell deformation, drug sensitivity, effects of molecular alterations, and tumor-host interaction. Many colors of fluorescent proteins are now known and can be used to color code cancer cells of a specific genotype or phenotype. Upon co-implantation in a single animal, the interaction between the variants can be visualized. For example, a highly metastatic variant can be labeled with GFP, and its low metastatic variant can be labeled with red

fluorescent protein (RFP). The host and the tumor can be differentially labeled with fluorescent proteins. The host mouse can be a transgenic organism expressing GFP in all of its cells or specifically in cells of interest such as endothelial cells. The GFP-expressing mice can be transplanted with cells expressing RFP. Interaction of the tumor cells with the host cells can then be imaged. Cells themselves can be double labeled with GFP in the nucleus and RFP in the cytoplasm. With such double-labeled cells, nuclear-cytoplasmic dynamics can be imaged. These uses of fluorescent proteins are the subject of this review. In addition to cancer, many other processes can be visualized *in vivo* with fluorescent proteins including gene expression,[4] infection,[5] and behavior of stem cells.[6,7]

1.3 Whole-body Imaging with Fluorescent Proteins

The first use of GFP for whole-body imaging was by Yang et al., who visualized primary and metastatic tumor growth in real time.[4,8] The intrinsic brightness of fluorescent proteins enables cells to be visualized inside intact animals by whole-body imaging. GFP-expressing primary and metastatic tumor growth could be visualized by whole-body imaging in numerous organs.[8]

An RFP-expressing human pancreatic tumor cell line was introduced as tissue fragments into the pancreases of nude mice by surgical orthotopic implantation (SOI). As the tumors were growing, whole-body optical imaging was used to track, in real time, the growth of the primary tumor and the formation of metastatic lesions that developed in the spleen, bowel, portal lymph nodes, omentum, and liver. The images were used for quantification of tumor growth in each of these organs.[9] Tumor area measured by GFP imaging correlated with tumor volume measured in the opened animal, which validated the use of whole-body imaging to quantitate tumor growth and metastasis. Whole-body imaging with this model

Address all correspondence to Robert M. Hoffman, AntiCancer, Inc., 7917 Ostrow St., San Diego, CA 92111. Tel: (858)654–2555; Fax: (858)268–4175; E-mail: all@anticancer.com

was used to compare standard and experimental agents for pancreatic cancer.[10,11]

Peyruchaud and colleagues[12] established a GFP-expressing bone-metastasis subclone of MDA-MB-231 (B02/GFP.2) by repeated *in vivo* passages in bone by use of the heart injection model. When injected into the tail vein of mice, the selected cells grew preferentially in bone. Whole-body fluorescence imaging of the live mice showed that bone metastases could be detected about 1 week before radiologically distinctive osteolytic lesions developed. Furthermore, when the tumor-bearing mice were treated with a bisphosphonate, progression of established osteolytic lesions and the expansion of breast cancer cells within bone, were inhibited. Using whole-body GFP imaging, Peyruchaud et al.[13] showed that the angiogenesis inhibitor angiostatin greatly inhibited tumor growth in bone by inhibiting osteoclast activity.

Using a different approach, human ovarian tumor cells (SKOV3.ip1) were made to express GFP by infection with a replication-deficient adenoviral (Ad) vector encoding GFP.[14] The infected cells showed high GFP fluorescence, and when implanted into mice, intraperitoneal tumors as small as 0.2 mm in diameter could be detected by whole-body imaging within 24 hours.[15]

In another study,[16] however, GFP-expressing tumors could not be detected by whole-body imaging until 7 days after subcutaneous (sc) tumor cell inoculation. These results strongly contrast with the results described above. This discrepancy shows the need to use appropriate instrumentation and techniques for whole-body fluorescence imaging.

Transgene expression in intact animals can be visualized by whole-body imaging. GFP expressed in the cells of brain, liver, pancreas, prostate, and bone was visualized by whole-body imaging. Both nude and normal mice were labeled by directly injecting adenoviral GFP. Within 5–8 h after adenoviral GFP injection, the fluorescence of the expressed GFP in brain and liver became visible, and whole-body images were recorded at video rates. The GFP fluorescence continued to increase for at least 12 h and remained detectable in liver for up to 4 months. The method requires only that the expressed gene or promoter be fused or operatively linked to GFP.[4]

Angiogenesis can be whole-body imaged with fluorescent proteins in GFP-expressing tumors; the nonluminous induced capillaries generated from the host are clearly visible against the very bright tumor fluorescence when examined by whole-body imaging. Whole-body imaging of tumor angiogenesis was demonstrated by injecting GFP-expressing Lewis lung carcinoma cells into the sc site of the footpad of nude mice. The footpad is relatively transparent, with comparatively few resident blood vessels, allowing quantitative imaging of tumor angiogenesis in the intact animal. Capillary density increased linearly over a 10-day period as determined by whole-body imaging. Similarly, the GFP-expressing human breast tumor MDA-MB-435 was orthotopically transplanted to the mouse fat pad, where whole-body optical imaging showed that blood vessel density increased linearly over a 20-week period. The GFP-expressing angiogenesis mouse models can be used for real-time *in vivo* evaluation of agents inhibiting or promoting tumor angiogenesis in physiological microenvironments.[17]

In another approach, Yu et al.[18] have shown that GFP-expressing bacteria injected intravenously into live animals entered and replicated in solid tumors and metastases. The tumor-specific amplification process was visualized in real time using GFP fluorescence, which revealed the locations of the tumors and metastases. Localization of tumors was visualized by the GFP expressed by the emitting microorganisms in immunocompetent and in immunocompromised rodents with syngeneic and allogeneic tumors.

A genetically-modified bacteria strain, *Salmonella typhimurium* A1, auxotrophic for Leu and Arg, was labeled with GFP. The GFP-expressing bacteria grew in the cytoplasm of PC-3 human prostate cancer cells and caused nuclear destruction. These effects were visualized in cancer cells labeled with GFP in the nucleus and RFP in the cytoplasm. *In vivo*, the bacteria caused tumor inhibition and regression of xenografts visualized by whole-body imaging with the PC-3 prostate cancer cells labeled with RFP grafted into nude mice. The GFP bacteria continued to proliferate in the PC-3 tumor, which stopped growing, but did not continuously grow in normal tissue.[19]

Opening a reversible skin flap in the light path markedly reduces signal attenuation, increasing detection sensitivity many-fold. The observable depth of tissue is thereby greatly increased. For example, GFP-expressing pancreatic tumors and their angiogenic microvessels were externally imaged by means of a peritoneal-wall skin flap.[20]

The above results demonstrate that whole-body imaging with GFP can allow cancer growth progression and metastasis to be visualized in real time even at the cellular level. This new technology can be used to understand cancer as a continuing process and to rapidly screen for new drugs.

1.4 How Does In Vivo Imaging with Fluorescent Proteins Work? Is Autofluorescence a Problem?

The beauty of fluorescent proteins is their brightness, multiple colors with distant spectra, and simplicity of use. The intrinsic fluorescence is so bright that very simple equipment can be used for many *in vivo* studies of tumor growth and metastasis, drug sensitivity, and angiogenesis. The strong signal from the fluorescent proteins readily distinguishes it from autofluorescence of the skin or other organs. For screening for large changes in fluorescence and other macro imaging studies, equipment as simple as LED flashlights with an appropriate excitation filter and a simple emission filter are sufficient (see Fig. 1).[21]

To consistently produce metastasis in mice, the genetically-fluorescent tumors should be transplanted orthotopically.[17,22–31] Once the fluorescent protein-expressing tumors have developed and metastases have formed, individual tumor cells can be detected in the live mouse by use of external imaging with fairly simple equipment. A fluorescence light box with fiber-optic lighting at about 490 nm and appropriate filters, placed on top of the light box, can be used to image large tumors and can be viewed with the naked eye.[8] Alternatively, the light box can be linked to a camera with an appropriate filter to enable images to be displayed on a monitor and digitally stored.[8] In order to visualize smaller tumors and metastases, the animal can be put on a fluorescence dissecting microscope that incorporates a light source and filters for excitation at about 490 nm. Fluorescence emission can be observed through a 520-nm long-pass filter.[8] The animals can
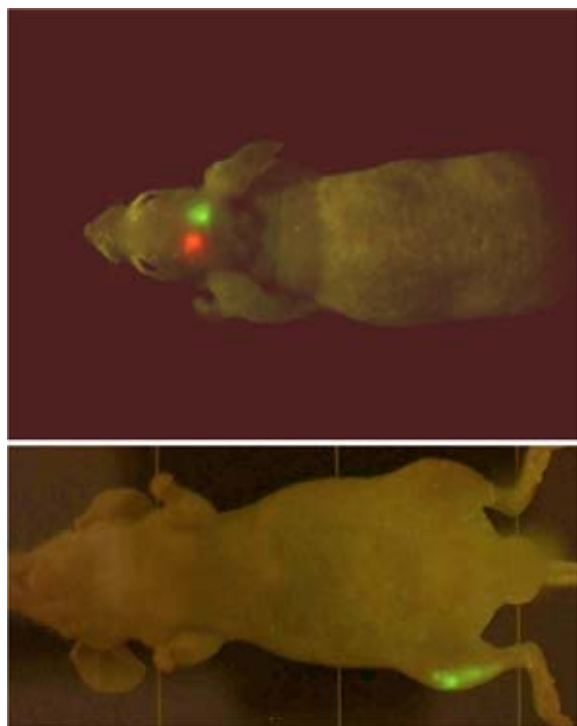
Fig. 1 Whole-body imaging of GFP and RFP tumors in nude mice. (a) GFP- and RFP-expressing tumors implanted on the brain in a single nude mouse. The excitation light was produced with a simple blue-LED flashlight equipped with an excitation filter with a central peak of 470 nm. The image was acquired with a Hamamatsu CCD camera. (b) GFP-expressing tumor implanted in the tibia of the right hind leg of a nude mouse imaged with the blue-LED flashlight as in (a).[21]

be irradiated at 490 nm for long periods without harming them or bleaching the GFP or RFP fluorescence. Images can be processed with standard software and the imaging procedures can be repeated as often as necessary without harming the animal.[20]

More highly sophisticated equipment including highly sensitive color CCD cameras as well as dual-photon lasers can be used for ultra-high-resolution *in vivo* imaging of fluorescent protein expression.[32] Software has been developed that can automatically identify areas of fluorescence in the animals and quantify the fluorescent area and intensity.

The use of tunable filters allows the isolation of any individual spectrum in any fluorescent pixel. This technique eliminates autofluorescence as well as enabling high-resolution spectral distinction when multiple fluorescent proteins are being used or when the fluorescence signal eminates from deep in the animal. Spectral resolution enables, for example, high-resolution whole-body visualization of tumor blood vessels.[33]

1.5 Imaging GFP Tumor Cells in and around Blood Vessels

Following injection of tumor cells stably expressing GFP into the tail vein of mice, it was possible to visualize single tumor cells in blood vessels.[22] Huang,[34] Li,[35] and their respective co-workers visualized GFP tumor-cell–vessel interaction by use of skin window chambers in rodents and observed angio-

genic effects very early in tumor colony formation. When as few as 60–80 tumor cells were present, increased vasodilation and vessel morphology changes were observed. When as few as 100 cells were present, neovascularization was induced. Moore and colleagues have also visualized vessels in a GFP-expressing rodent cell line.[36] Al-Mehdi et al.[37] and Wong et al.[38] observed the steps in early hematogenous metastasis of tumor cells expressing GFP in subpleural microvessels in intact, perfused mouse and rat lungs. Metastatic tumor cells attached to the endothelia of pulmonary precapillary arterioles and capillaries. Extravasation of tumor cells was rare. Early tumor colony formation was observed entirely within the blood vessels.

Rat tongue carcinoma cell lines expressing GFP have been used to investigate the formation of micrometastasis. The cells were injected into the portal vein and then tracked by use of intravital video microscopy.[39] The two cell types—LM-GFP metastatic and E2-GFP nonmetastatic tongue carcinoma cells—immediately got stuck in the sinusoidal vessels near terminal portal venules. The E2-GFP cells disappeared from the liver sinusoid within 3 days, whereas a substantial number of LM-GFP cells remained in the liver—possibly because these cells formed stable attachments to the sinusoidal wall. Upon examination of the process with a confocal laser scanning microscope, only LM-GFP cells were shown to grow in the liver.

Mook et al.[40] noted that initial arrest of colon cancer cells in sinusoids of the liver was due to size restriction after injection of the CC531S-GFP rat tumor cell line.

Sturm et al.[41] injected GFP-expressing mouse colon tumor 26 cells into the spleen of immunocompetent BALB/c mice. Some of the tumor cells were trapped in presinusoidal vasculature as well as in the sinusoids. Some of the tumor cells were attached to the vessel wall and some were seen to extravasate.

Wang et al.[42] visualized the trafficking of metastatic cells targeting the liver via the portal vein using GFP-expressing cancer cells. Within 72 h after transplantation on the ascending colon in nude mice, metastasis was visualized *ex vivo* on a single-cell basis around the portal vein by GFP imaging.

Brown et al.[32] showed that multiphoton laser-scanning microscopy could provide high-resolution three-dimensional images of angiogenesis-related gene expression and that this technique could be used to investigate deeper regions of GFP-expressing tumors in dorsal skin-fold chambers. To monitor the activity of the vascular endothelial growth factor (VEGF) promoter, Fukumura et al.[43,44] made transgenic mice that express GFP under control of the VEGF promoter. Multiphoton laser scanning microscopy showed that the tumor was able to induce activity of the VEGF promoter and subsequent vessel formation. Yang et al.[17] observed angiogenesis by whole-body imaging in GFP-expressing tumors. The vessels were observed by contrast to the fluorescent tumor.

Wong and colleagues[45] showed that death of transformed, metastatic, rat embryo cells, which were expressing GFP, occurred via apoptosis in the lungs 24−48 h after injection into the circulation. BCL-2 over-expression conferred apoptosis resistance for 24−48 h after injection. This inhibition of apoptosis led to a greater number of macroscopic metastases.

Chang and co-workers[46] used CD31 and CD105 to identify endothelial cells and GFP-labeling to identify tumor cells.

These studies showed that colon carcinoma xenografts had mosaic vessels with focal regions where no CD31/CD105 immunoreactivity was detected and tumor cells appeared to contact the vessel lumen.

Wyckoff et al.[47] used metastatic (MTLn3) and nonmetastatic (MTC) cell lines derived from the rat mammary adenocarcinoma 13762 NF, expressing GFP, to measure tumor cell density in the blood, individual tumor cells in the lungs, and lung metastases. Metastatic cells showed greater orientation toward blood vessels whereas nonmetastatic cells fragment when interacting with vessels. A major difference in intravasation between metastatic and nonmetastatic cells was thus visualized by GFP in the primary tumor.

Ahmed et al.[48] used transgenic mice expressing GFP driven by the mouse mammary virus promoter (MMTV). This model was used for imaging of transgenic mammary tumors and metastases at the single cell level of resolution.

Glinskii et al.[49] reported here that GFP-expressing human prostate carcinoma growing orthotopically efficiently deliver viable metastatic cells to the host circulation. This is in contrast to the ectopic tumors of the same lineage, which do not deliver live cells into the circulation. Coinjection of an equivalent mixture of isolated and cultured circulating GFP-expressing clones and parental RFP-expressing human prostate carcinoma cells revealed that the selected GFP-labeled viable circulating cells have an increased metastatic propensity relative to the RFP-labeled parental cells. The identification and isolation of highly malignant viable circulating human prostate carcinoma cells from orthotopic but not ectopic models suggests the tumor microenvironment plays a very important role in enabling metastasis to occur. Berezovskaya et al.[50] have now demonstrated that the metastatic human prostate carcinoma cells selected for survival in the circulation have increased resistance to anoikis, which is apoptosis induced by cell detachment. Increased expression of the apoptosis inhibitory protein XIAP contributes to this anoikis resistance of the circulating metastatic human prostate carcinoma cells and thereby contributes to their ability to form distant metastasis.

1.6 Visualizing Cellular and Nuclear Deformation and Dynamics in Brain Blood Vessels

Yamamoto et al.[51] have genetically engineered dual-color fluorescent cells with one color in the nucleus and the other in the cytoplasm that enable real-time nuclear-cytoplasmic dynamics to be visualized in living cells *in vivo* as well as *in vitro* (see Fig 2). Nuclear GFP expression enabled visualization of nuclear dynamics, whereas simultaneous cytoplasmic RFP expression enabled visualization of nuclear-cytoplasmic ratios as well as simultaneous cell and nuclear shape changes. Common-carotid artery injection of dual-color cells and a reversible skin flap enabled the external visualization of the dual-color cells in capillaries in the mouse brain where extreme elongation of the cell body as well as the nucleus occurred in order for the tumor cells to enter the capillaries.

1.7 Imaging Tumor Cell Deformation and Migration in Blood Vessels of Live Mice in Real Time

Tumor cells expressing GFP in the nucleus and RFP in the cytoplasm were injected in the heart of nude mice. A skin flap
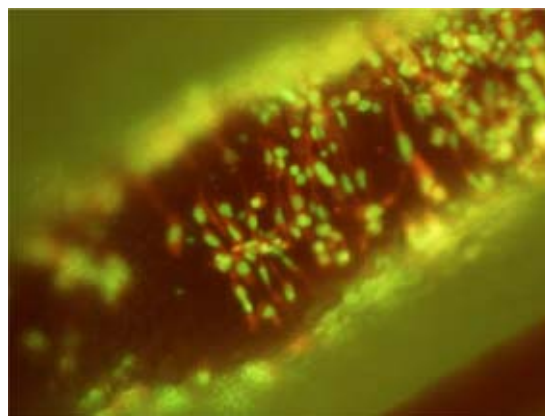

Fig. 2 Intravital image of Lewis lung carcinoma cells labeled with GFP in the nucleus by linkage of GFP with histone H2B and labeled with RFP in the cytoplasm with a retrovirus. The double-labeled carcinoma cells are surrounding a blood vessel after the cells have extravasated. Imaging is with an Olympus OV100 whole mouse imaging system in a living mouse (K. Yamauchi and R. M. Hoffman, unpublished data).

on the abdomen was made and spread on a flat stand. Highly elongated cancer cells in capillaries in the skin flap in living mice were visualized. The cells in the capillaries elongated to fit the width of these vessels. The average length of the major axis of the cancer cells in the capillaries increased to 3.97 times their normal length. The nuclei increased their length 1.64 times in the capillaries. Cancer cells that were arrested in capillaries over 8 μm in diameter could migrate up to 48.3 μm/h. The data suggest that the minimum diameter of capillaries where cancer cells are able to migrate is approximately 8 μm. Dual-color cells could be visualized in larger vessels as well with an occasional cell extravasating.[52] Extravasated cancer cells were also visualized to become intimately involved with blood vessels (K. Yamauchi and R. M. Hoffman, unpublished results). Fluorescent protein imaging can visualize in real time the cellular and nuclear dynamics of tumor cells within and associated with blood vessels.

1.8 Color Coding Cancer Cells

Yamamoto et al.[53] described use of GFP-labeled or RFP-labeled HT-1080 human fibrosarcoma cells to determine clonality by simple fluorescence visualization of metastatic colonies after mixed implantation in severe combined immunodeficient (SCID) mice of the red and green fluorescent cells. Resulting pure red or pure green colonies were scored as clonal, whereas mixed yellow colonies were scored as nonclonal. In a spontaneous metastasis model originating from footpad injection in SCID mice, 95% of the resulting lung colonies were either pure green or pure red, indicating monoclonal origin, whereas 5% were of mixed color, indicating polyclonal origin. In an experimental lung metastasis model established by tail vein injection in SCID mice, clonality of lung metastasis was dependent on cell number. Experiments with color coded cells will enable differentially labeled tumor cells of different phenotype and/or genotype and follow their behavior in the same animal.

1.9 Imageable Tumor-host Models

A transgenic GFP nude mouse with ubiquitous GFP expression has been developed. The GFP nude mouse was obtained by crossing nontransgenic nude mice with the transgenic C57/B6 mouse in which the β-actin promoter drives GFP expression in essentially all tissues.[54] In the adult mice, the organs all brightly expressed GFP, including the heart, lungs, spleen, pancreas, esophagus, stomach, and duodenum. The skinned skeleton highly expressed GFP. Pancreatic islets showed GFP fluorescence. The spleen cells were also GFP positive. Red fluorescent protein (RFP)-expressing human cancer cell lines, including PC-3-RFP prostate cancer, HCT-116-RFP colon cancer, MDA-MB-435-RFP breast cancer, and HT1080-RFP fibrosarcoma, were transplanted to the transgenic GFP nude mice. All of these human tumors grew extensively in the transgenic GFP nude mice.[55] These models show the details of the tumor-stroma interaction, especially tumor-induced angiogenesis and tumor-infiltrating lymphocytes. The GFP-expressing tumor vasculature, both nascent and mature, of the GFP host mouse, could be readily distinguished interacting with the RFP-expressing tumor cells. GFP-expressing dendritic cells were observed contacting RFP-expressing tumor cells with their dendrites. GFP-expressing macrophages were observed engulfing RFP-expressing cancer cells. GFP lymphocytes were seen surrounding cells of the RFP tumor.[56] With fluorescent protein imaging we are now able to visualize the cell-cell interactions of tumor and stroma in the living state.

Li et al.[6] and Amoh et al.[7] have shown that the neural-stem cell marker nestin is expressed in hair follicle stem cells and the blood vessel network interconnecting hair follicles in the skin of transgenic mice with nestin-regulatory-element-driven GFP (ND-GFP). The hair follicles were shown to give rise to ND-GFP blood vessels in the skin. Tumor angiogenesis was visualized by dual-color fluorescence imaging in ND-GFP transgenic mice after transplantation of the murine melanoma cell line B16F10 expressing RFP. ND-GFP was highly expressed in proliferating endothelial cells and nascent blood vessels in the growing tumor. Results of immunohistochemical staining showed that the blood-vessel-specific antigen CD31 was expressed in ND-GFP-expressing nascent blood vessels. Progressive angiogenesis during tumor growth was readily visualized during tumor growth by GFP expression. RFP tumor cells were visualized inside ND-GFP blood vessels. Doxorubicin inhibited the nascent tumor angiogenesis as well as tumor growth in ND-GFP mice transplanted with B16F10-GFP.[57] These new dual-color imageable models of tumor angiogenesis enable new insights into this process.

Duda et al.[58] noted at the time of transplantation, tumor fragments contain "passenger" cells: endothelial cells and other stromal cells from the original host. They investigated the fate of GFP labeled endothelial and nonendothelial stromal cells after transplantation in syngeneic mice. Angiogenic stroma associated with tumor or adipose tissue persisted when transplanted, remained functional, and governed the initial neovascularization of grafted tissue fragments for more than 4 weeks after implantation. The passenger endothelial cells survived longer than other stromal cells, which are replaced by host-activated fibroblasts after 3 weeks. The transplantability of tumor stroma suggests that the angiogenic potential of a tumor xenograft depends on the presence of passenger endothelial cells and other stromal cells within the xenograft.

1.10 Unique Features of In Vivo GFP Imaging

The GFP approach has several important advantages over other optical approaches to imaging. In comparison with the luciferase reporter, GFP has a much stronger signal and therefore can be used to image unrestrained animals. The fluorescence intensity of GFP is very strong since the quantum yield is about 0.9.[59–63] The protein sequence of GFP has also been "humanized," which enables it to be highly expressed in mammalian cells.[64] In addition, GFP fluorescence is fairly unaffected by the external environment since the chromaphore is protected by the three-dimensional structure of the protein.[65] The excitation wavelength is quite long at 490 nm,[60–63] which does not quench the fluorescence and therefore long-term measurements can be made. In vivo, GFP fluorescence is mainly limited by light scattering which, as noted above, can be overcome by spectral resolution,[33] skin flaps,[20] and endoscopes,[66–68] such that single cells can be imaged externally. Longer wavelength fluorescence proteins, such as RFP, can also be used to reduce scatter.

An improved method of whole-body GFP imaging made use of a laser excitation source and band-pass filters matched specifically to GFP and constitutive tissue fluorescence emission bands. Processing of the primary GFP fluorescence images acquired by the CCD camera subtracted background tissue autofluorescence. This approach achieved 100% sensitivity and specificity for in vivo detection of 10%-transfected BxPc3-GFP pancreatic tumor cells after subcutaneous grafting or orthotopic implantation in the pancreas of nude mice.[69]

The luciferase reporter technique requires that animals are anesthetized and restrained so that sufficient photons to construct an image can be collected. Furthermore, this process must be carried out in a virtually light-free environment and animals must be injected with the luciferin substrate, which has to reach every tumor cell in order to be useful. The clearance of the luciferin also results in an unstable luciferase signal.[70] These limitations preclude studies that would be perturbed by anesthesia, restraint, or substrate injection and also makes high-throughput screening unfeasible. Expression of firefly luciferase (Luc) can be used to visualize tumor growth and regression in response to various therapies in mice. However, detection of Luc-labeled cells in vivo was limited to at least 1,000 human tumor cells.[71,72] Real images are not produced. Instead, pseudocolor images indicating photon counts are seen. Thus, cellular or subcellular imaging has not been achieved with luciferase as has been done with fluorescent proteins. The high-intensity signal produced by GFP allows unrestrained animals to be imaged without any perturbation or substrate—irradiation with nondamaging blue light is the only step needed. Images can be captured with fairly simple apparatus and there is no need for total darkness.

A fusion vector harboring the Renilla luciferase gene, a reporter gene encoding a monomeric RFP, and a mutant herpes simplex virus type thymidine kinase was tested in vivo. A highly sensitive cooled charge-coupled device camera compatible with both luciferase and fluorescence imaging compared these two signals from the fused reporter gene using a

lentivirus vector in 293T cells implanted in nude mice. The signal from RFP was approximately 1000 times stronger than luciferase.[73] Since the two proteins were transcribed from the same promoter, these data suggest similar numbers of molecules of each in the cells, further emphasizing the relative brightness of fluorescent proteins.

Near-infrared probes activated by the action of proteases[74–76] can also be used for optical imaging of tumors. This approach requires substrate injection and the tumor must contain a specific protease that cleaves the substrate. Tumors on normal tissues such as the liver that also contain these proteases cannot be visualized because background signals are too high. Structural data has shown that fragmentation of the chromophore is an intrinsic, autocatalytic step toward the formation of the mature chromophore of the photoactivitable *Anemonia sulcata*-GFP.[79]

A mutant of the *Anemonia sulcata* chromoprotein (asCP) has been generated. The mutant protein is capable of irreversible photoconversion from the nonfluorescent to a stable bright-red fluorescent form ("kindling"). This "kindling fluorescent protein" (KFP1) can be used for precise *in vivo* photolabeling to track the movements of cells, organelles, and proteins.[77]

A dual-color monomeric protein, photoswitchable cyan fluorescent protein (PS-CFP) has been described. PS-CFP is capable of efficient photoconversion from cyan to green, changing both its excitation and emission spectra in response to 405-nm light irradiation. Complete photoactivation of PS-CFP results in a 1,500-fold increase in the green-to-cyan fluorescence ratio. PS-CFP was used as a photoswitchable tag to study trafficking of the human dopamine transporter in living cells.[78]

Recently, a GFP has been cloned from a coral that has the property of sensitive and reversible wavelength-dependent on-off switching. This switchable GFP has been shown to be useful for studying protein trafficking between nucleus and cytoplasm.[80] Future studies could use the switchable GFPs *in vivo*.

As mentioned above, a transgenic GFP nude mouse with ubiquitous GFP expression has been developed. In the adult mice, the organs all brightly express GFP. RFP-expressing human cancer cell lines grew extensively in the transgenic GFP nude mouse.[55] This dual-color model shows the details of the tumor-stroma interaction, especially tumor-induced angiogenesis and tumor-infiltrating lymphocytes. Recently, Vintersten et al.[81] reported the development of an RFP-expressing transgenic mouse with expression in many tissues. A variant of DSRed, DSRedT3 was used to develop the ES cells to make this transgenic mouse. The availability of GFP and RFP transgenic mice gives rise to the possibility of GFP-RFP chimeric mice to color code host cells with specific genes of interest that could control specific aspects of host control of tumor growth and progression. Their effects could then be imaged upon transplantation of specific tumor types, which would fluoresce a third color.

A GFP-transgenic rat has recently been developed using the CAG promoter. GFP expression in brain, lung, liver, and islet tissues was restricted to early developmental stages, but it was continuously strong in the exocrine pancreas, kidney, and cardiac and skeletal muscles.[82]

An albumin enhancer/promoter-driven Alb-DsRed2 transgenic rat has now been developed that expresses DsRed2 in hepatolyses. To study the transdifferentiation of bone marrow cells into albumin producing cells, bone marrow cells from the Alb-DsRed2 Tg rat were injected into rats having acute and chronic liver damage. DsRed2-positive cells were generated in the recipient liver after bone marrow injection thereby visualizing the differentiation of bone marrow cells into hepatocytes.[83]

1.11 Are Fluorescent Protein-expressing Cells More Antigenic than Parental Cells?

A syngenic murine colon carcinoma cell line (colon 26 cells) was transfected with enhanced green fluorescent protein (EGFP). The transfected cells maintained the highly malignant attributes of the wild-type cells. Following injection into the portal circulation of Balb/c-mice, liver metastases occur in the same time span for both parental and GFP cells, indicating no immune reaction against the GFP-expressing cells.[41,84]

Using a syngeneic mouse model harboring primary, genetically-modified myc-driven lymphomas expressing GFP, whole-body imaging showed that disruption of apoptosis downstream of p53 by Bcl-2 confers a highly aggressive phenotype, metastatic throughout the mouse body.[85] The myc-driven GFP-expressing lymphomas with p53 or INK4a/ARF mutations or overexpressed Bcl-2 respond poorly to cyclophosphamide therapy *in vivo* compared to wild type cells as shown by whole-body imaging.[86] No immune reactions against the GFP cells were observed in this syngeneic system either.

B16F0-GFP mouse melanoma cells were injected into the tail vein or portal vein of 6-week-old C57BLy6. Whole-body optical images showed metastatic lesions in the brain, liver, and bone of B16F0-GFP, again suggesting no immune reaction against the GFP-expressing cells.[8]

A syngeneic model of the Lewis lung carcinoma in which the carcinoma cells are labeled with GFP was established. The tumor cells were transplanted on the dorsal side of the ear of C57-B16 mice in order to give the tumor cells access to the lymphatic system. This model of the Lewis lung carcinoma extensively metastasized to numerous lymph nodes throughout the body of the animal as well as visceral organs as visualized by fluorescence microscopy using the bright GFP signal. Twenty-one different metastatic sites, including lymph nodes throughout the body, were identified among the cohort of transplanted animals. The data demonstrate a predilection of the Lewis lung carcinoma for lymphatic pathways of metastasis throughout the animal body. This syngeneic model again demonstrates no immune reaction against the GFP-expressing tumor cells.[87]

These studies strongly indicate that GFP-expressing cells are not more immunogenic than parental cells and therefore GFP is not particularly antigenic.

2 Conclusions

Tumor cells stably expressing GFP and other fluorescent proteins *in vivo* are a powerful new tool for cancer research. Stability of expression has been studied by Naumov et al.[88] who noted that all the CHO-K1-GFP cells used in their study were stably fluorescent (measured by flow cytometry) even

after 24 days of growth in medium where they were deprived of selective pressure. This finding implies that GFP can be stably expressed in cells *in vivo*. This feature has proved true for all cells studied so far in our laboratories and is exemplified by the generation of extensive GFP-expressing metastases.

The use of GFP-expressing tumor cells in fresh tissue, or live animals,[3,8,20,22,23,88] has provided new insights into the real-time growth and metastatic behavior of cancer. Several independent studies, which include an extensive comparison between metastases of GFP-transduced carcinoma and the parental cell lines,[41,89,90] have shown that GFP or RFP transduction and expression does not affect metastatic behavior including syngeneic models.[41] These studies indicate that GFP expression does not demonstrably affect immunogenicity of the cells.

GFP can be transfected into any cell type of interest and used as a cytoplasmic marker to show the general outlines of cells *in vivo* and fine morphological details such as long slender pseudopodial projections.[88] Cells which express GFP in the nucleus and RFP in the cytoplasm offer even more cellular details *in vivo*.

The development of tumor cells that stably express GFP at high levels has enabled investigation of tumor and metastatic growth in a completely noninvasive manner by use of whole-body imaging.[8] For the first time, tumor growth and metastatic studies, including drug evaluations, can be done and quantified in real time in nonpeturbed individual animals. The potential of this technology is very high.

A further advantage of GFP-expressing cells is the increased contrast between brightly fluorescent tumor tissue and blood vessels within it. The ability to visualize and quantify blood-vessel development in metastases *in vivo* will greatly facilitate studies of angiogenesis and the testing of effects of antiangiogenic agents on metastatic development.[17,20,88]

A transgenic GFP nude mouse with ubiquitous GFP expression has been developed. In the adult mice, the organs all brightly express GFP. RFP-expressing human cancer cell lines grew extensively in the transgenic GFP nude mouse.[55] This dual-color model shows the details of the tumor-stroma interaction, especially tumor-induced angiogenesis and tumor-infiltrating lymphocytes. Red fluorescent protein transenic rodents have now been developed, opening the possibility of multicolor normal chimeras as well as tumor-host chimeras.[83]

The GFP approach has several important advantages over other optical approaches to imaging. In comparison with the luciferase reporter, GFP has a much stronger signal and therefore can be used to image unrestrained animals. The fluorescence intensity of GFP is very strong since the quantum yield is about 0.9.[59–63] The protein sequence of GFP has also been "humanized," which enables it to be highly expressed in mammalian cells.[64] In addition, GFP fluorescence is fairly unaffected by the external environment since the chromaphore is protected by the three-dimensional structure of the protein.[65] The excitation wavelength is quite long at 490 nm,[60–63] which does not quench the fluorescence and therefore long-term measurements can be made. *In vivo*, GFP fluorescence is mainly limited by light scattering which, as noted above, can be overcome by spectral resolution,[33] skin flaps,[20] and endoscopes,[66–68] such that single cells can be imaged exter-

nally. Longer wavelength fluorescence proteins, such as RFP, can also be used to reduce scatter.

An improved method of whole-body GFP imaging made use of a laser excitation source and bandpass filters matched specifically to GFP and constitutive tissue fluorescence emission bands. Processing of the primary GFP fluorescence images acquired by the CCD camera subtracted background tissue autofluorescence. This approach achieved 100% sensitivity and specificity for *in vivo* detection of 10%-transfected BxPc3-GFP pancreatic tumor cells after subcutaneous grafting or orthotopic implantation in the pancreas of nude mice.[69]

The luciferase reporter technique requires that animals are anesthetized and restrained so that sufficient photons to construct an image can be collected. Furthermore, this process must be carried out in a virtually light-free environment and animals must be injected with the luciferin substrate, which has to reach every tumor cell in order to be useful. The clearance of the luciferin also results in an unstable luciferase signal.[70] These limitations preclude studies that would be perturbed by anesthesia, restraint, or substrate injection and also makes high-throughput screening unfeasible. Expression of firefly luciferase (Luc) can be used to visualize tumor growth and regression in response to various therapies in mice but has not been applicable to cellular visualization, since real images are not generated. Detection of Luc-labeled cells *in vivo* was limited to at least 1,000 human tumor cells.[71,72] The high intensity signal produced by GFP, in contrast, allows unrestrained animals to be imaged without any perturbation or substrate—irradiation with nondamaging blue light is the only step needed. Images can be captured with fairly simple apparatus and there is no need for total darkness.

A comparison of luciferase and fluorescence imaging compared a fused luciferase-GFP lentivirus and showed that RFP was approximately 1,000 times stronger than luciferase.[73]

Near-infrared probes activated by the action of proteases[74–76] require substrate injection, and the tumor must contain a specific protease that cleaves the substrate. Tumors on normal tissues such as the liver that also contain these proteases cannot be visualized, because background signals are too high.

Fluorescent protein imaging is enabling not only whole-body imaging but, due to its cellular resolution and multiple colors, is giving rise to a new field of *in vivo* cell biology.

2.1 Future Directions

The applications of *in vivo* cellular imaging with fluorescent proteins should markedly expand with the development of proteins with new colors. Shaner et al.[91] have taken the *Discosoma* RFP and converted it through multiple amino acid substitutions into a monomer. With further genetic modification this group has created from the *Discosoma* RFP monomer a series of modified proteins with multiple new colors from yellow-orange to red-orange. These new colored proteins include mBanana, mOrange, dTomato, tdTomato, mTangerine, mStrawberry, and mCherry with increasingly longer emission maxima. It is expected that many additional colored proteins will be isolated from various organisms and modified to produce even more colors. The availability of a large number of different colored proteins will enable simultaneous imaging of

multiple cellular events *in vivo*, surpassing what can be visualized both *in vivo* as well as *in vitro* today.

These switchable GFPs that can either be kindled and/or extinguished or change colors have been shown to be useful for studying protein trafficking between nucleus and cytoplasm.[80] Future studies could use the switchable GFPs *in vivo*.

The availability of GFP and RFP transgenic rodents[81,83] gives rise to the possibility of GFP-RFP chimeras. Such chimeras could be used to color-code host cells that effect tumor growth and progression. Their effects could then be imaged upon transplantation of specific tumor types, which would fluoresce a third color.

Ilyin and co-workers visualized glioma cells in rats by inserting a fiber-optic endoscope through a pre-implanted guide cannula. Tumor monitoring was coupled to confocal microscopy so that visualization of the fluorescent signals from the C-6 glioma-GFP cells that had been preimplanted in the brain was very sensitive.[66] Funovics et al.[92] described the design and construction of a miniaturized multichannel near infrared endoscopic imaging system developed for high-resolution imaging of mice. This endoscope was used to visualize tumor cells transplanted orthotopically in mice. The developed device should be useful for *in vivo* imaging using fluorescent proteins.[67] Stanziale et al.[68] showed the herpes-simplex virus NV1066-expressing GFP can be used to assess oncolytic therapy in a minimally invasive laparoscopic system in mouse models of gastric cancer. After intraperitoneal administration of NV1066-GFP, macroscopic tumor foci begin to express GFP visualized by direct laparoscopy with the appropriate fluorescent filters. Noncancerous organs were not infected and did not express GFP. Thus, GFP expression in intraperitoneal tumors can be visualized laparoscopically, allowing detection and localization of viral gene therapy.

Endoscopy and laporoscopy offer real possibilities of clinical application of fluorescent protein imaging. Detection of single cancer cells will become possible in patients. Futuristic applications could include implantation of micro light sources and detectors which could signal external detectors of the presence of a single new fluorescent cancer cell growing in the patient.

A fluorescence system for studying protein dynamics in mitosis has been established in a human cell line expressing histone H3 and truncated importin α as fusions to cyan fluorescent protein (CFP) and RFP, respectively, to visualize the chromosomes and the nuclear envelope in living cells, respectively.[93] This is a further development to apply to the new field of *in vivo* cell biology that can visualize nuclear and chromatin changes during cancer progression.

References

1. V. Verkhusha and K. A. Lukyanov, "The molecular properties and applications of Anthozoa fluorescent proteins and chromoproteins," *Nat. Biotechnol.* **22**, 289–296 (2004).
2. M. Zimmer, "Green fluorescent protein (GFP): Applications, structure and related photophysical behavior," *Chem. Rev. (Washington, D.C.)* **102**, 759–781 (2002).
3. T. Chishima, Y. Miyagi, X. Wang, H. Yamaoka, H. Shimada, A. R. Moossa, and R. M. Hoffman, "Cancer invasion and micrometastasis visualized in live tissue by green fluorescent protein expression," *Cancer Res.* **57**, 2042–2047 (1997).
4. M. Yang, E. Baranov, A. R. Moossa, S. Penman, and R. M. Hoffman, "Visualizing gene expression by whole-body fluorescence imaging," *Proc. Natl. Acad. Sci. U.S.A.* **97**, 12278–12282 (2000).
5. M. Zhao, M. Yang, E. Baranov, X. Wang, S. Penman, A. R. Moossa, and R. M. Hoffman, "Spatial-temporal imaging of bacterial infection and antibiotic response in intact animals," *Proc. Natl. Acad. Sci. U.S.A.* **98**, 9814–9818 (2001).
6. L. Li, J. Mignone, M. Yang, M. Matic, S. Penman, G. Enikolopov, and R. M. Hoffman, "Nestin expression in hair follicle sheath progenitor cells," *Proc. Natl. Acad. Sci. U.S.A.* **100**, 9958–9961 (2003).
7. Y. Amoh, L. Li, M. Yang, A. R. Moossa, K. Katsuoka, S. Penman, and R. M. Hoffman, "Nascent blood vessels in the skin arise from nestin-expressing hair follicle cells," *Proc. Natl. Acad. Sci. U.S.A.* **101**, 13291–13295 (2004).
8. M. Yang, E. Baranov, P. Jiang, F.-X. Sun, X.-M. Li, L. Li, S. Hasegawa, M. Bouvet, M. Al-Tuwaijri, T. Chishima, H. Shimada, A. R. Moossa, S. Penman, and R. M. Hoffman, "Whole-body optical imaging of green fluorescent protein-expressing tumors and metastases," *Proc. Natl. Acad. Sci. U.S.A.* **97**, 1206–1211 (2000).
9. M. H. Katz, S. Takimoto, D. Spivack, A. R. Moossa, R. M. Hoffman, and M. Bouvet, "A novel red fluorescent protein orthotopic pancreatic cancer model for the preclinical evaluation of chemotherapeutics," *J. Surg. Res.* **113**, 151–160 (2003).
10. M. H. Katz, M. Bouvet, S. Takimoto, D. Spivack, A. R. Moossa, and R. M. Hoffman, "Survival efficacy of adjuvant cytosine-analogue CS-682 in a fluorescent orthotopic model of human pancreatic cancer," *Cancer Res.* **64**, 1828–1833 (2004).
11. M. H. Katz, M. Bouvet, S. Takimoto, D. Spivack, A. R. Moossa, and R. M. Hoffman, "Selective antimetastatic activity of cytosine analog CS-682 in a red fluorescent protein orthotopic model of pancreatic cancer," *Cancer Res.* **63**, 5521–5525 (2003).
12. O. Peyruchaud, B. Winding, I. Pecheur, C. M. Serre, P. Delmas, and P. Clezardin, "Early detection of bone metastases in a murine model using fluorescent human breast cancer cells: application to the use of the bisphosphonate zoledronic acid in the treatment of osteolytic lesions," *J. Bone Miner. Res.* **16**, 2027–2034 (2001).
13. O. Peyruchaud, C.-M. Serre, R. NicAmhlaoibh, P. Fournier, and P. Clezardin, "Angiostatin inhibits bone metastasis formation in nude mice through a direct anti-osteoclastic activity," *J. Biol. Chem.* **278**, 45826–45832 (2003).
14. T. R. Chaudhuri, J. M. Mountz, B. E. Rogers, E. E. Partridge, and K. R. Zinn, "Light-based imaging of green fluorescent protein-positive ovarian cancer xenografts during therapy," *Gynecol. Oncol.* **82**, 581–589 (2001).
15. T. R. Chaudhuri, Z. Cao, V. N. Krasnykh, A. V. Stargel, N. Belousova, E. E. Partridge, and K. R. Zinn, "Blood-based screening and light based imaging for the early detection and monitoring of ovarian cancer xenografts," *Technol. Cancer Res. Treat.* **2**, 171–180 (2003).
16. G. Choy, S. O'Connor, F. E. Diehn, N. Costouros, H. R. Alexander, P. Choyke, and S. K. Libutti, "Comparison of noninvasive fluorescent and bioluminescent small animal optical imaging," *BioTechniques* **35**, 1022–1026 (2003); **35**, 1028–1030 (2003).
17. M. Yang, E. Baranov, X. M. Li, J. W. Wang, P. Jiang, L. Li, A. R. Moossa, S. Penman, and R. M. Hoffman, "Whole-body and intravital optical imaging of angiogenesis in orthotopically implanted tumors," *Proc. Natl. Acad. Sci. U.S.A.* **98**, 2616–2621 (2001).
18. Y. A. Yu, S. Shabahang, T. M. Timiryasova, Q. Zhang, R. Beltz, I. Gentschev, W. Goebel, and A. A. Szalay, "Visualization of tumors and metastases in live animals with bacteria and vaccinia virus encoding light-emitting proteins," *Nat. Biotechnol.* **22**, 313–320 (2004).
19. M. Zhao, M. Yang, X.-M. Li, P. Jiang, E. Baranov, S. Li, M. Xu, S. Penman, and R. M. Hoffman, "Tumor-targeting bacterial therapy with amino acid auxotrophs of GFP-expressing *Salmonella typhimurium*," *Proc. Natl. Acad. Sci. U.S.A.* **102**, 755–760 (2005).
20. M. Yang, E. Baranov, J.-W. Wang, P. Jiang, X. Wang, F.-X. Sun, M. Bouvet, A. R. Moossa, S. Penman, and R. M. Hoffman, "Direct external imaging of nascent cancer, tumor progression, angiogenesis, and metastasis on internal organs in the fluorescent orthotopic model," *Proc. Natl. Acad. Sci. U.S.A.* **99**, 3824–3829 (2002).
21. M. Yang, G. Luiken, E. Baranov, and R. M. Hoffman, "Facile whole-body imaging of internal fluorescent tumors in mice with an LED flashlight," *BioTechniques* **39**, 170–172 (2005).
22. T. Chishima, Y. Miyagi, X. Wang, E. Baranov, Y. Tan, H. Shimada, A. R. Moossa, and R. M. Hoffman, "Metastatic patterns of lung cancer visualized live and in process by green fluorescent protein expression," *Clin. Exp. Metastasis* **15**, 547–552 (1997).

23. T. Chishima, Y. Miyagi, X. Wang, Y. Tan, H. Shimada, A. R. Moossa, and R. M. Hoffman, "Visualization of the metastatic process by green fluorescent protein expression," *Anticancer Res.* **17**, 2377–2384 (1997).

24. M. Yang, S. Hasegawa, P. Jiang, X. Wang, Y. Tan, T. Chishima, H. Shimada, A. R. Moossa, and R. M. Hoffman, "Widespread skeletal metastatic potential of human lung cancer revealed by green fluorescent protein expression," *Cancer Res.* **58**, 4217–4221 (1998).

25. B. Rashidi, M. Yang, P. Jiang, E. Baranov, Z. An, X. Wang, A. R. Moossa, and R. M. Hoffman, "A highly metastatic Lewis lung carcinoma orthotopic green fluorescent protein model," *Clin. Exp. Metastasis* **18**, 57–60 (2000).

26. R. H. Hastings, D. W. Burton, R. A. Quintana, E. Biederman, A. Gujral, and L. J. Deftos, "Parathyroid hormone-related protein regulates the growth of orthotopic human lung tumors in athymic mice," *Cancer* **92**, 1402–1410 (2001).

27. M. Yang, P. Jiang, F. X. Sun, S. Hasegawa, E. Baranov, T. Chishima, H. Shimada, A. R. Moossa, and R. M. Hoffman, "A fluorescent orthotopic bone metastasis model of human prostate cancer," *Cancer Res.* **59**, 781–786 (1999).

28. H. Maeda, T. Segawa, T. Kamoto, H. Yoshida, A. Kakizuka, O. Ogawa, and Y. Kakehi, "Rapid detection of candidate metastatic foci in the orthotopic inoculation model of androgen-sensitive prostate cancer cells introduced with green fluorescent protein," *Prostate* **45**, 335–340 (2000).

29. M. Bouvet, M. Yang, S. Nardin, X. Wang, P. Jiang, E. Baranov, A. R. Moossa, and R. M. Hoffman, "Chronologically-specific metastatic targeting of human pancreatic tumors in orthotopic models," *Clin. Exp. Metastasis* **18**, 213–218 (2000).

30. M. Bouvet, J. Wang, S. R. Nardin, R. Nassirpour, M. Yang, E. Baranov, P. Jiang, A. R. Moossa, and R. M. Hoffman, "Real-time optical imaging of primary tumor growth and multiple metastatic events in a pancreatic cancer orthotopic model," *Cancer Res.* **62**, 1534–1540 (2002).

31. M. Yang, T. Chishima, X. Wang, E. Baranov, H. Shimada, A. R. Moossa, and R. M. Hoffman, "Multi-organ metastatic capability of Chinese hamster ovary cells revealed by green fluorescent protein (GFP) expression," *Clin. Exp. Metastasis* **17**, 417–422 (1999).

32. E. B. Brown, R. B. Campbell, Y. Tsuzuki, L. Xu, P. Carmeliet, D. Fukumura, and R. K. Jain, "*In vivo* measurement of gene expression, angiogenesis and physiological function in tumors using multiphoton laser scanning microscopy," *Nat. Med.* **7**, 864–868 (2001).

33. R. Levenson, M. Yang, and R. M. Hoffman, "Whole-body dual-color differential fluorescence imaging of tumor angiogenesis enhanced by spectral unmixing," *Proc. Am. Assoc. Cancer Res.* **45**, 46 (Abstract #202) (2004).

34. M. S. Huang, T. J. Wang, C. L. Liang, H. M. Huang, I. C. Yang, H. Yi-Jan, and M. Hsiao, "Establishment of fluorescent lung carcinoma metastasis model and its real-time microscopic detection in SCID mice," *Clin. Exp. Metastasis* **19**, 359–368 (2002).

35. C.-Y. Li, S. Shan, Q. Huang, R. D. Braun, J. Lanzen, K. Hu, P. Lin, and M. W. Dewhirst, "Initial stages of tumor cell-induced angiogenesis: evaluation via skin window chambers in rodent models," *J. Natl. Cancer Inst.* **92**, 143–147 (2000).

36. A. Moore, E. Marecos, M. Simonova, R. Weissleder, and A. Bogdanov, Jr., "Novel gliosarcoma cell line expressing green fluorescent protein: a model for quantitative assessment of angiogenesis," *Microvasc. Res.* **56**, 145–153 (1998).

37. A. B. Al-Mehdi, K. Tozawa, A. B. Fisher, L. Shientag, A. Lee, and R. J. Muschel, "Intravascular origin of metastasis from the proliferation of endothelium-attached tumor cells: a new model for metastasis," *Nat. Med.* **6**, 100–102 (2000).

38. C. W. Wong, C. Song, M. M. Grimes, W. Fu, M. W. Dewhirst, R. J. Muschel, and A. B. Al-Mehdi, "Intravascular location of breast cancer cells after spontaneous metastasis to the lung," *Am. J. Pathol.* **161**, 749–753 (2002).

39. S. Ito, H. Nakanishi, Y. Ikehara, T. Kato, Y. Kasai, K. Ito, S. Akiyama, A. Nakao, and M. Tatematsu, "Real-time observation of micrometastasis formation in the living mouse liver using a green fluorescent protein gene-tagged rat tongue carcinoma cell line," *Int. J. Cancer* **93**, 212–217 (2001).

40. O. R. Mook, J. Van Marle, H. Vreeling-Sindelarova, R. Jonges, W. M. Frederiks, and C. J. Van Noorden, "Visualization of early events in tumor formation of eGFP-transfected rat colon cancer cells in liver," *Hepatology* **38**, 295–304 (2003).

41. J. W. Sturm, M. A. Keese, B. Petruch, R. G. Bonninghoff, H. Zhang, N. Gretz, M. Hafner, S. Post, and R. S. McCuskey, "Enhanced green fluorescent protein-transfection of murine colon carcinoma cells: Key for early tumor detection and quantification," *Clin. Exp. Metastasis* **20**, 395–405 (2003).

42. J.-W. Wang, M. Yang, and R. M. Hoffman, "Visualizing portal vein metastatic trafficking to the liver with green fluorescent protein-expressing tumor cells," *Anticancer Res.* **24**, 3699–3702 (2004).

43. D. Fukumura, F. Yuan, W. L. Monsky, Y. Chen, and R. K. Jain, "Effect of host microenvironment on the microcirculation of human colon adenocacinoma," *Am. J. Pathol.* **151**, 679–688 (1997).

44. D. Fukumura, R. Xavier, T. Sugiura, Y. Chen, E. C. Park, N. Lu, M. Selig, G. Nielsen, T. Taksir, R. K. Jain, and B. Seed, "Tumor induction of VEGF promoter activity in stromal cells," *Cell* **94**, 715–725 (1998).

45. C. W. Wong, A. Lee, L. Shientag, J. Yu, Y. Dong, G. Kao, A. B. Al-Mehdi, E. J. Bernhard, and R. J. Muschel, "Apoptosis: an early event in metastatic inefficiency," *Cancer Res.* **61**, 333–338 (2001).

46. Y. S. Chang, E. di Tomaso, D. M. McDonald, R. Jones, R. K. Jain, and L. L. Munn, "Mosaic blood vessels in tumors: frequency of cancer cells in contact with flowing blood," *Proc. Natl. Acad. Sci. U.S.A.* **97**, 14608–14613 (2000).

47. J. B. Wyckoff, J. G. Jones, J. S. Condeelis, and J. E. Segall, "A critical step in metastasis: *in vivo* analysis of intravasation at the primary tumor," *Cancer Res.* **60**, 2504–2511 (2000).

48. F. Ahmed, J. Wyckoff, E. Y. Lin, W. Wang, Y. Wang, L. Hennighausen, J. Miyazaki, J. Jones, J. W. Pollard, J. S. Condeelis, and J. E. Segall, "GFP expression in the mammary gland for imaging of mammary tumor cells in transgenic mice," *Cancer Res.* **62**(24), 7166–7169 (2002).

49. A. B. Glinskii, B. A. Smith, P. Jiang, X. M. Li, M. Yang, R. M. Hoffman, and G. V. Glinsky, "Viable circulating metastatic cells produced in orthotopic but not ectopic prostate cancer models," *Cancer Res.* **63**, 4239–4243 (2003).

50. O. Berezovskaya, A. D. Schimmer, A. B. Glinskii, C. Pinilla, R. M. Hoffman, J. C. Reed, and G. V. Glinky, "Increased expression of apoptosis inhibitor protein XIAP contributes to anoikis resistance of circulating human prostate metastasis precursor cancer cells," *Cancer Res.* **65**, 2378–2386 (2005).

51. N. Yamamoto, P. Jiang, M. Yang, M. Xu, K. Yamauchi, H. Tsuchiya, K. Tomita, G. M. Wahl, A. R. Moossa, and R. M. Hoffman, "Cellular dynamics visualized in live cells *in vitro* and *in vivo* by differential dual-color nuclear-cytoplasmic fluorescent-protein expression," *Cancer Res.* **64**, 4251–4256 (2004).

52. K. Yamauchi, M. Yang, P. Jiang, N. Yamamoto, M. Xu, Y. Amoh, K. Tsuji, M. Bouvet, H. Tsuchiya, K. Tomita, A. R. Moossa, and R. M. Hoffman, "Real-time *in vivo* dual-color imaging of intracapillary cancer cell and nucleus deformation and migration," *Cancer Res.* **65**, 4246–4252 (2005).

53. N. Yamamoto, M. Yang, P. Jiang, M. Xu, H. Tsuchiya, K. Tomita, A. R. Moossa, and R. M. Hoffman, "Determination of clonality of metastasis by cell-specific color-coded fluorescent-protein imaging," *Cancer Res.* **63**, 7785–7790 (2003).

54. M. Okabe, M. Ikawa, K. Kominami, T. Nakanishi, and Y. Nishimune, " 'Green mice' as a source of ubiquitous green cells," *FEBS Lett.* **407**, 313–319 (1997).

55. M. Yang, J. Reynoso, P. Jiang, L. Li, A. R. Moossa, and R. M. Hoffman, "Transgenic nude mouse with ubiquitous green fluorescent protein expression as a host for human tumors," *Cancer Res.* **64**, 8651–8656 (2004).

56. M. Yang, L. Li, P. Jiang, A. R. Moossa, S. Penman, and R. M. Hoffman, "Dual-color fluorescence imaging distinguishes tumor cells from induced host angiogenic vessels and stromal cells," *Proc. Natl. Acad. Sci. U.S.A.* **100**, 14259–14262 (2003).

57. Y. Amoh, L. Li, M. Yang, P. Jiang, A. R. Moossa, K. Katsuoka, and R. M. Hoffman, "Hair-follicle-derived blood vessels vascularize tumors in skin and are inhibited by doxorubicin," *Cancer Res.* **65**, 2337–2343 (2005).

58. D. G. Duda, D. Fukumura, L. L. Munn, M. F. Booth, E. B. Brown, P. Huang, B. Seed, and R. K. Jain, "Differential transplantability of tumor-associated stromal cells," *Cancer Res.* **64**, 5920–5924 (2004).

59. J. Morin and J. Hastings, "Energy transfer in a bioluminescent system," *J. Cell Physiol.* **77**, 313–318 (1971).

60. B. Cormack, R. Valdivia, and S. Falkow, "FACS-optimized mutants of the green fluorescent protein (GFP)," *Gene* **173**, 33–38 (1996).

61. A. Crameri, E. A. Whitehorn, E. Tate, and W. P. C. Stemmer, "Improved green fluorescent protein by molecular evolution using DNA shuffling," *Nat. Biotechnol.* **14**, 315–319 (1996).

62. S. Delagrave, R. E. Hawtin, C. M. Silva, M. M. Yang, and D. C. Youvan, "Red-shifted excitation mutants of the green fluorescent protein," *Bio/Technology* **13**, 151–154 (1995).

63. R. Heim, A. B. Cubitt, and R. Y. Tsien, "Improved green fluorescence," *Nature* **373**, 663–664 (1995).

64. S. Zolotukhin, M. Potter, W. W. Hauswirth, J. Guy, and N. Muzyczka, "A 'humanized' green fluorescent protein cDNA adapted for high-level expression in mammalian cells," *J. Virol.* **70**, 4646–4654 (1996).

65. C. W. Cody, D. C. Prasher, W. M. Westler, F. G. Prendergast, and W. W. Ward, "Chemical structure of the hexapeptide chromophore of the Aequorea green fluorescent protein," *Biochemistry* **32**, 1212–1218 (1993).

66. S. E. Ilyin, M. C. Flynn, and C. R. Plata-Salaman, "Fiber-optic monitoring coupled with confocal microscopy for imaging gene expression *in vitro* and *in vivo*," *J. Neurosci. Methods* **108**, 91–96 (2001).

67. K. Kelly, H. Alencar, M. Funovics, U. Mahmood, and R. Weissleder, "Detection of invasive colon cancer using a novel, targeted, library-derived fluorescent peptide," *Cancer Res.* **64**, 6247–6251 (2004).

68. S. F. Stanziale, B. M. Stiles, A. Bhargava, S. A. Kerns, N. Kalakonda, and Y. Fong, "Oncolytic herpes simplex virus-1 mutant expressing green fluorescent protein can detect and treat peritoneal cancer," *Hum. Gene Ther.* **15**, 609–618 (2004).

69. S. Wack, A. Hajri, F. Heisel, M. Sowinska, C. Berger, M. Whelan, J. Marescaux, and M. Aprahamian, "Feasibility, sensitivity, and reliability of laser-induced fluorescence imaging of green fluorescent protein-expressing tumors *in vivo*," *Mol. Ther.* **7**, 765–773 (2003).

70. J. S. Burgos, M. Rosol, R. A. Moats, V. Khankaldyyan, D. B. Kohn, M. D. Nelson, Jr., and W. E. Laug, "Time course of bioluminescent signal in orthotopic and heterotopic brain tumors in nude mice," *BioTechniques* **34**, 1184–1188 (2003).

71. T. J. Sweeney, V. Mailander, A. A. Tucker, A. B. Olomu, W. Zhang, Y. Cao, R. S. Negrin, and C. H. Contag, "Visualizing the kinetics of tumor-cell clearance in living animals," *Proc. Natl. Acad. Sci. U.S.A.* **96**, 12044–12049 (1999).

72. C. H. Contag, D. Jenkins, P. R. Contag, and R. S. Negrin, "Use of reporter genes for optical measurements of neoplastic disease *in vivo*," *Neoplasia* **2**, 41–52 (2000).

73. P. Ray, A. De, J.-J. Min, R. Y. Tsien, and S. S. Gambhir, "Imaging tri-fusion multimodality reporter gene expression in living subjects," *Cancer Res.* **64**, 1323–1330 (2004).

74. R. Weissleder, C. H. Tung, U. Mahmood, and A. Bogdanov, Jr., "*In vivo* imaging of tumors with protease-activated near-infrared fluorescent probes," *Nat. Biotechnol.* **17**, 375–378 (1999).

75. C. Bremer, C. H. Tung, and R. Weissleder, "*In vivo* molecular target assessment of matrix metalloproteinase inhibition," *Nat. Med.* **7**, 743–748 (2001).

76. T. Jiang, E. S. Olson, Q. T. Nguyen, M. Roy, P. A. Jennings, and R. Y. Tsien, "Tumor imaging by means of proteolytic activation of cell-penetrating peptides," *Proc. Natl. Acad. Sci. U.S.A.* **101**, 17867–17872 (2004).

77. D. M. Chudakov, V. V. Belousov, A. G. Zaraisky, V. V. Novoselov, D. B. Staroverov, D. B. Zorov, S. Lukyanov, and K. A. Lukyanov, "Kindling fluorescent proteins for precise *in vivo* photolabeling," *Nat. Biotechnol.* **21**, 191–194 (2003).

78. D. M. Chudakov, V. V. Verkhusha, D. B. Staroverov, E. A. Souslova, S. Lukyanov, and K. A. Lukyanov, "Photoswitchable cyan fluorescent protein for protein tracking," *Nat. Biotechnol.* **22**, 1435–1439 (2004).

79. P. G. Wilmann, J. Petersen, R. J. Devenish, M. Prescott, and J. Rossjohn, "Variations on the GFP Chromophore: A polypeptide fragmentation within the chromophore revealed in the 2.1-a crystal structure of a nonfluorescent chromoprotein from anemonia sulcata," *J. Biol. Chem.* **280**, 2401–2404 (2005).

80. R. Ando, H. Mizuno, and A. Miyawaki, "Regulated fast nucleocytoplasmic shuttling observed by reversible protein highlighting," *Science* **306**, 1370–1373 (2004).

81. K. Vintersten, C. Monetti, M. Gertsenstein, P. Zhang, L. Laszlo, S. Biechele, and A. Nagy, "Mouse in red: Red fluorescent protein expression in mouse ES cells, embryos, and adult animals," *Genesis* **40**, 241–246 (2004).

82. K. Takeuchi, A. Sereemaspun, T. Inagaki, Y. Hakamata, T. Kaneko, T. Murakami, M. Takahashi, E. Kobayashi, and S. Ookawara, "Morphologic characterization of green fluorescent protein in embryonic, neonatal, and adult transgenic rats," *Anat. Rec. A. Discov. Mol. Cell Evol. Biol.* **274**, 883–886 (2003).

83. Y. Sato, Y. Igarashi, Y. Hakamata, T. Murakami, T. Kaneko, M. Takahashi, N. Seo, and E. Kobayashi, "Establishment of Alb-DsRed2 transgenic rat for liver regeneration research," *Biochem. Biophys. Res. Commun.* **311**, 478–481 (2003).

84. J. W. Sturm, R. Magdeburg, K. Berger, B. Petruch, S. Samel, R. Bonninghoff, M. Keese, M. Hafner, and S. Post, "Influence of TNFA on the formation of liver metastases in a syngenic mouse model," *Int. J. Cancer* **107**, 11–21 (2003).

85. C. A. Schmitt, J. S. Fridman, M. Yang, E. Baranov, R. M. Hoffman, and S. W. Lowe, "Dissecting p53 tumor suppressor functions *in vivo*," *Cancer Cell* **1**, 289–298 (2002).

86. C. A. Schmitt, J. S. Fridman, M. Yang, S. Lee, E. Baranov, R. M. Hoffman, and S. W. Lowe, "Senescence program controlled by p53 and p16^INK4a contributes to the outcome of cancer therapy," *Cell* **109**, 335–346 (2002).

87. V. Bobek, K. Kolostov, D. Pinterov, M. Boubelik, P. Jiang, M. Yang, and R. M. Hoffman, "Syngeneic lymph-node-targeting model of green fluorescent protein-expressing Lewis lung carcinoma," *Clin. Exp. Metastasis* **21**, 705–708 (2004).

88. G. N. Naumov, S. M. Wilson, I. C. MacDonald, E. E. Schmidt, V. L. Morris, A. C. Groom, R. M. Hoffman, and A. F. Chambers, "Cellular expression of green fluorescent protein, coupled with high-resolution *in vivo* videomicroscopy, to monitor steps in tumor metastasis," *J. Cell. Sci.* **112**, 1835–1842 (1999).

89. K. L. Farina, J. B. Wyckoff, J. Rivera, H. Lee, J. E. Segall, J. S. Condeelis, and J. G. Jones, "Cell motility of tumor cells visualized in living intact primary tumors using green fluorescent protein," *Cancer Res.* **58**, 2528–2532 (1998).

90. J.-Y. Lu, H. C. Chen, R. Y. Chu, T. C. Lin, P. I. Hsu, M. S. Huang, C. J. Tseng, and M. Hsiao, "Establishment of red fluorescent protein-tagged HeLa tumor metastasis models: determination of DsRed2 insertion effects and comparison of metastatic patterns after subcutaneous, intraperitoneal, or intravenous injection," *Clin. Exp. Metastasis* **20**, 121–133 (2003).

91. N. C. Shaner, R. E. Campbell, P. A. Steinbach, B. N. Giepmans, A. E. Palmer, and R. Y. Tsien, "Improved monomeric red, orange and yellow fluorescent proteins derived from *Discosoma* sp. red fluorescent protein," *Nat. Biotechnol.* **22**, 1567–1572 (2004).

92. M. A. Funovics, H. Alencar, H. S. Su, K. Khazaie, R. Weissleder, and U. Mahmood, "Miniaturized multichannel near infrared endoscope for mouse imaging," *Molecular Imaging* **2**, 350–357 (2003).

93. T. Fukada, K. Inoue, T. Urano, and K. Sugimoto, "Visualization of chromosomes and nuclear envelope in living cells for molecular dynamics studies," *BioTechniques* **37**, 552–556 (2004).